

# Preparation of heterogeneous Fenton-Type nano catalysts and their application to methylene blue degradation

Co Thanh Thien<sup>1,2,\*</sup>, Le Dinh Khoi<sup>1</sup>, Doan Thi Nhu Thuy<sup>1</sup>, Le Van De<sup>1</sup>



Use your smartphone to scan this QR code and download this article

## ABSTRACT

**Introduction:** Iron-based nanocatalysts are known as a new generation heterogeneous Fenton catalyst, replacing the traditional Fenton catalyst system which has many disadvantages in experimental processes and industrial applications. In this study, we focused on the preparation of iron nanoparticles and their use when embedded in traditional supports, as well as tested their catalytic activity by modified Fenton-type oxidation of methylene blue (MB) substrate. **Method:** Scanning Electron Microscope (SEM), Transmission Electron Microscopy (TEM), X-ray diffraction (XRD) and UV-vis were used for physio-chemical characterization of the catalysts. **Results:** Iron nanoparticles were obtained in the reduction of iron salt by sodium borohydride (NaBH<sub>4</sub>), with particle size in the range of 4-5 nm. Fe-X (X represents C, Bentonite, Al<sub>2</sub>O<sub>3</sub>, or ZnO) was synthesized in high yield and applied to the Fenton oxidation of MB; approximately 99% conversion was observed in the case of Fe-C. **Conclusion:** Supported iron nanoparticles are active catalysts for the oxidation of MB; however, there are limitations if pH is above 3.

**Key words:** Fenton, nanocatalyst, iron catalyst, oxidation, water treatment

## INTRODUCTION

In recent years, wastewater containing synthetic dyes has garnered increased attention due to factors such as continuous discharge, low toxicity and biodegradability<sup>1,2</sup>. Specifically, the oxidation of methylene blue (MB) and basic dyes of thiazine are receiving greater interest. Therefore, treatment by Fenton method has been attracting many researchers<sup>3-6</sup>.

Iron-based nanocatalysts are known as a new generation heterogeneous Fenton catalyst which can replace the traditional Fenton catalyst system that has many disadvantages in experimental processes as well as in industrial applications<sup>7</sup>. Both heterogeneous and homogeneous Fenton catalysts show similar activity for the same amount of catalyst used. However, in the case of traditional Fenton catalysts, there is a need for a considerable amount of chemicals and manpower to remove the mixture containing the iron catalysts<sup>8</sup>. Therefore, in order to improve the Fenton process, a number of reports have used supported iron catalysts for applications in drug sciences<sup>9</sup>, treatment of heavy metal pollution<sup>10</sup>, chemical catalysis<sup>11</sup>, and industrial textile and dyes<sup>12</sup>.

Moreover, due to the reduction of metal, ethylene glycol (EG) reduction is a common process for the preparation of metal nanoparticles. In particular, with iron reduction, high temperature or microwave irradiation

is usually required to improve the reduction performance<sup>13,14</sup>. Sodium borohydride (NaBH<sub>4</sub>) is considered as a force reducing agent which can reduce ionic precursors at room temperature; a disadvantage of the NaBH<sub>4</sub> process, however, is the formation of irregular particle size<sup>15</sup>. Consequently, the combination of the EG and NaBH<sub>4</sub> processes can yield better reduction in the preparation of the nanoparticles.

In this study, we describe the preparation of iron nanoparticles and their use as a new catalyst and impregnated into traditional supports, as well as evaluate their catalytic activities by modified Fenton-type oxidation of MB substrate.

## MATERIALS - METHODS

### Materials

Unless otherwise noted, all procedures were carried out in air. Reagent grade iron(II) sulfate heptahydrate 99.5% (FeSO<sub>4</sub>·7H<sub>2</sub>O), ethylene glycol 99.5% (EG), methylene blue (MB), and sodium borohydride 98% (NaBH<sub>4</sub>) were purchased from Merck (Germany). Aluminum oxide (Al<sub>2</sub>O<sub>3</sub>), zinc oxide (ZnO), hydrogen peroxide (H<sub>2</sub>O<sub>2</sub>), and polyvinyl pyrrolidone-K30 (PVP) were purchased from various Chinese suppliers (Xilong, China). Binh Thuan bentonite (Bent) and activated carbon were purchased from local suppliers (Binh Thuan, Vietnam). Absolute ethanol and methanol were supplied by CHEMSOL (Ho Chi Minh city, Vietnam).

<sup>1</sup>University of Science, Ho Chi Minh City, Vietnam

<sup>2</sup>Vietnam National University, Ho Chi Minh City, Vietnam

### Correspondence

Co Thanh Thien, University of Science, Ho Chi Minh City, Vietnam

Vietnam National University, Ho Chi Minh City, Vietnam

Email: ctthien@hcmus.edu.vn

### History

- Received: 2020-08-28
- Accepted: 2020-11-02
- Published: 2020-12-02

DOI : 10.32508/stdj.v23i4.2451



### Copyright

© VNU-HCM Press. This is an open-access article distributed under the terms of the Creative Commons Attribution 4.0 International license.



**Cite this article :** Thien C T, Khoi L D, Thuy D T N, De L V. Preparation of heterogeneous Fenton-Type nano catalysts and their application to methylene blue degradation. *Sci. Tech. Dev. J.*; 23(4):769-775.

## Characterization

The morphology of iron catalysts was examined by scanning electron microscope (SEM) (Hitachi S4800, Japan). Transmission Electron Microscopy (TEM) images was collected using FEI Tecnai G2 F20 (University of Technology, Ho Chi Minh city). The X-ray diffraction (XRD) data of all samples were collected in a Philip X-Ray (Vietnam Petroleum Institute, Ho Chi Minh city) with Cu K $\alpha$  radiation running at 35 kV/30 mA in the 2 $\theta$  range 5°-75° with a step size of 0.2°/min. Nitrogen adsorption-desorption isotherms were collected at 77K using Brunauer-Emmett-Teller calculation (BET, AUTOSORB-1C Quantachrome); all samples were degassed at 100 °C and 10<sup>-6</sup> Pa. UV spectras were recorded on Agilent Cary 60 UV-Vis (Applied Physical Chemistry Laboratory of VNUHCM-University of Science, Ho Chi Minh city). Atomic Absorption pectroscopy (AAS) was analysed on Agilent 240AAS (Laboratory of Analysis-University of Science, Ho Chi Minh city). All the catalytic test were performed in a Multireactors Carousel 12 lus system (Laboratory of Catalysis-University of Science, Ho chi Minh city).

## Catalyst preparation

To a two-necked roundbottom flask, FeSO<sub>4</sub>.7H<sub>2</sub>O (0.5 g, 1.8 mmol) and 50 mL of deionized (DI) water were added. After stirring for 15 min, 25 mL of absolute ethanol and 1 g of PVP were added into the mixture. In another flask, a mixture of EG (2.0 mL) and NaBH<sub>4</sub> (0.1 g, 2.7 mmol) in 50 mL of DI water were prepared. Then, the reducing agent solution was added in a dropwise fashion to the mixture of iron salt, which was stirred until the solution appeared black. The iron nanoparticles were then loaded on the supports (X), such as Al<sub>2</sub>O<sub>3</sub>, bentonite, ZnO or activated carbon, under vacuum at room temperature. The process was repeated several times to make sure all the iron nanoparticles were loaded onto X.

## Catalyst evaluation

In this study, the activity of the catalyst was investigated via the degradation of MB under aqueous solution. The catalytic evaluation of Fe-X was carried out in a 20 mL multireactor with stirring at room temperature. In this process, 5.0 mol% of Fe-X was used in the MB aqueous solution of 40 mg/L (10 mL), and 1.0 mL of 30% hydrogen peroxide solution in water. The influence of pH on the process (at pH 3.0, 5.0, and 7.0) was observed by dosing hydrochloric acid. The concentration changes of MB were recorded by the colorimetric method at the maximum absorbance

of 664 nm. Reproducibility was checked by repeating the measurement several times and was found to be within acceptable limits.

## RESULTS

Iron nanoparticles were prepared by the reduction of FeSO<sub>4</sub>.7H<sub>2</sub>O using a combination of EG and NaBH<sub>4</sub> as reducing agent. The original blue solution turned dark when Fe<sup>0</sup> nanoparticles formed. The solution was then subjected to UV-Vis measurement.

**Figure 1** show the UV-Vis spectra of the iron nanoparticles prepared at room temperature. The absorption range of 300-320 nm was assigned for the absorption peaks of Fe<sup>2+</sup> and Fe<sup>3+</sup> ions. The solution of PVP did not absorb at the UV zone.

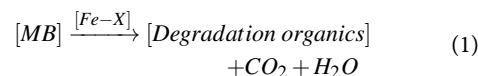
In addition, the solution of iron nanoparticles were further analyzed by TEM technique. TEM images were taken at 20 nm, 50 nm, and 100 nm. As illustrated in **Figure 3**, the average size of the iron nanoparticles was in the range of 4-5 nm.

According to AAS analysis, the concentration of supported iron nanoparticles as Fe-Al<sub>2</sub>O<sub>3</sub>, Fe-ZnO, Fe-Bent, and Fe-C were recorded at 14.20, 13.95, 12.00, and 10.77 wt%, respectively.

The surface morphology of Fe-X was characterized by SEM. As illustrated in **Figure 4**, the surface of Fe-Al<sub>2</sub>O<sub>3</sub> (A) showed uniform particles, with a number of spherical shape formed between the pores. Likewise, the surface of Fe-Bentonite (D) showed a similar morphology; both samples had similar specific surface area. In contrast, in the case of Fe-C (B), from the thickness of the slit-shaped pores which formed around the surface, it appeared that most of iron nanoparticles had not successfully attached to the activated carbon. Unfortunately, in the case of Fe-Bent (C), the surface was smooth, with a few pores, and with big cubic shapes covering the surface of the catalyst. It is worth noting that during the loading process, the spherical shape could be destroyed.

Moreover, **Table 1** indicates that the surface area of Fe-C was the highest compared to the other samples. In contrast, the surface of Fe-ZnO and Fe-Bent was smooth and had thin pores; thus the surface area was very low (approximately 28-42 m<sup>2</sup>.g<sup>-1</sup>). The supported iron nanoparticles did not have much of an effect on the surface area of the supports.

In order to evaluate the oxidation activity of the catalysts, 5.0 mol% of the Fe-X catalysts was used to oxidate MB solution in the presence of hydrogen peroxide. All experiments and results are summarized in **Figure 5**.



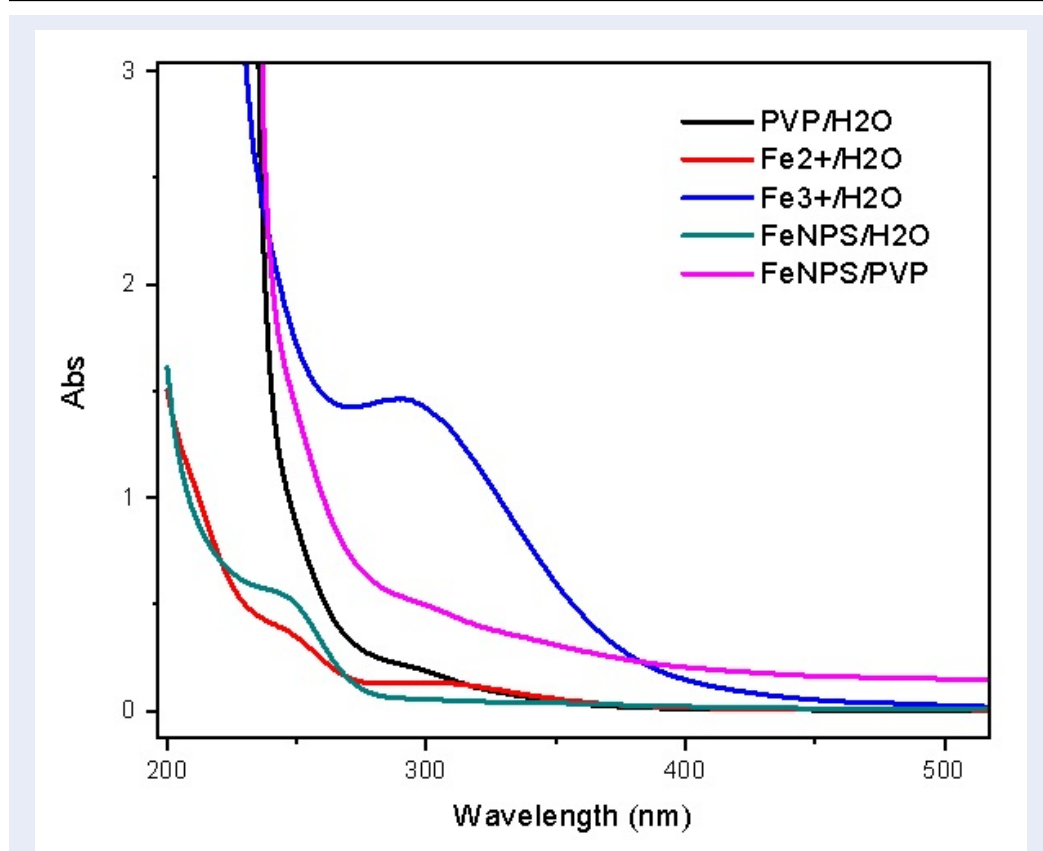


**Figure 1:** UV-vis absorbance spectra of the solution of iron nanoparticles which were reduced by a combination of EG and NaBH<sub>4</sub> at room temperature.

### DISCUSSION

According to H. Chen<sup>16</sup>, the characteristic spectra of iron nanoparticles are at two peaks,  $\lambda = 216$  nm and 268 nm. In **Figure 1**, an absorption peak at 268 nm was observed in the solution of iron nanoparticles, even if it was slightly smooth and seemed to be obscured. In addition, there was no absorption peaks of the Fe<sup>2+</sup> and Fe<sup>3+</sup> ions in this solution. This demonstrates that almost all Fe<sup>2+</sup> ion were successfully reduced to Fe<sup>0</sup> nanoparticles. This was also confirmed by XRD pattern in **Figure 2**, in which four cases showed the characteristic peak at  $2\theta$  angles of 44.9° (assigned for metallic iron), even though the peaks were rather weak due to the low concentration of iron nanoparticles in the samples.

As observed in **Figure 3**, the shape and size of the iron nanoparticles were determined to be spherical and in the range of 4-5 nm. These observations could be explained by the fact that the iron nanoparticles were protected and dispersed by the PVP molecules. Furthermore, the PVP molecules may have prevented the

**Table 1:** Specific surface areas of catalysts

Catalysts	S <sub>BET</sub> (m <sup>2</sup> .g <sup>-1</sup> )
Fe-Al <sub>2</sub> O <sub>3</sub>	69.98
Fe-C	224.69
Fe-ZnO	27.78
Fe-Bentonite	41.81

agglutination and deposition of the iron nanoparticles.

The catalytic oxidation exhibited an excellent decomposition of MB, as shown in **Figure 5**. All the iron-supported samples exhibited high activities, in particular Fe-C, which had the highest surface area and showed the best conversion (up to 99.7% in the case of pH 3). On the other hand, the influence of pH was also observed. For example, the conversion of MB was decreased when pH was increased to neutral. In the case of the Fe-ZnO catalyst, the conversion was decreased to 84.8% at pH 7, whereas it increased to 90.2% and 97.9% conversion at pH 5 and

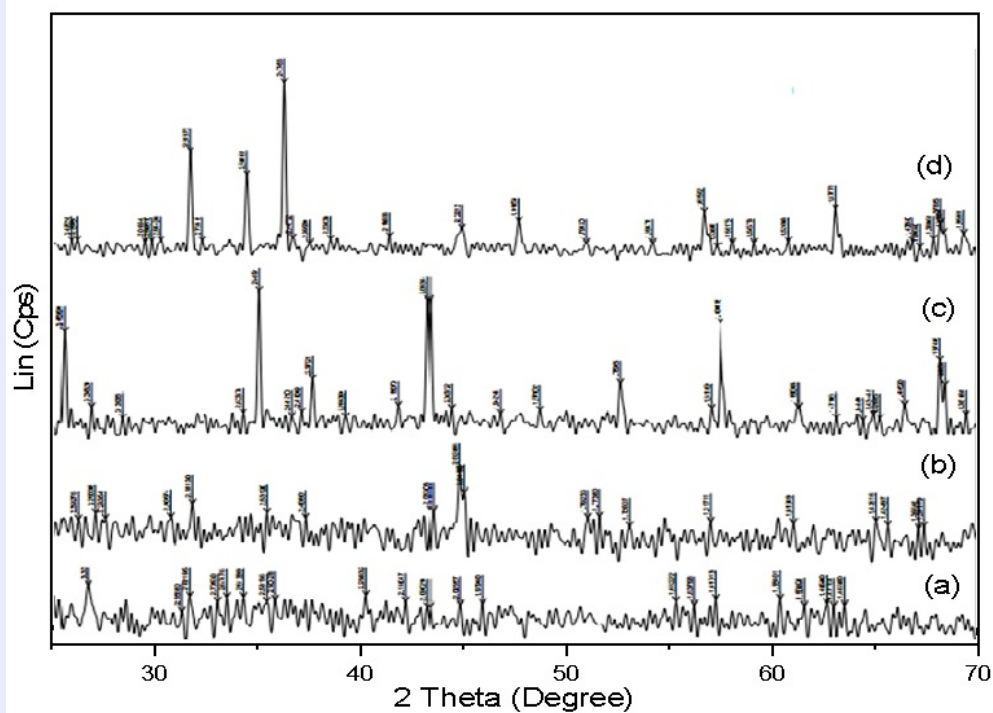


**Figure 2:** XRD patterns of: A) Fe-Bentonite, B) Fe-C, C) Fe-Al<sub>2</sub>O<sub>3</sub>, and D) Fe-ZnO; all were dried at 60 °C under vacuum for 8 h.

pH 3, respectively. It could be explained that in acidic environment, iron nanoparticles are more easily oxidized to iron ions, which play an important role in the Fenton-type heterogeneous catalysis<sup>17</sup>. Likewise, in the case of other samples, the MB conversion decreased to 89.2% and 78.9% at pH 7, as was the case with Fe-C and Fe-Bent catalysts, respectively. However, it was still lower than that at pH 5 for the conversion of 95.6% (Fe-C) and 86.7% (Fe-Bent). It is clear that in the case of pH 5, a moderate conversion was obtained. In order to propose the specific mechanism (Equation (1)), we may need to further investigate the kinetics reaction. The present catalysts- with their stability and activities- are potentially the most promising candidate for application in water pollution treatment.

## CONCLUSION

This study prepared and characterized Fe-X particles (X = C, Bentonite, Al<sub>2</sub>O<sub>3</sub>, or ZnO) as catalysts. All the physio-chemical characterization of the catalysts were evaluated in detail. All the results corroborated with the loading process. Indeed, XRD and TEM analyses indicated that iron was incorporated as Fe<sup>0</sup> inside X. Moreover, the catalytic test indicated that almost all

the supported iron nanoparticles exhibited high catalytic activities, especially at pH 3 where the conversion of MB reached 99.7% with the Fe-C catalyst.

## ABBREVIATIONS

Bent: bentonites  
 DI: deionized  
 EG: ethylene glycol  
 MB: methylene blue  
 PVP: polyvinyl pyrrolidone-K30  
 Zeolit: zeolites

## COMPETING INTERESTS

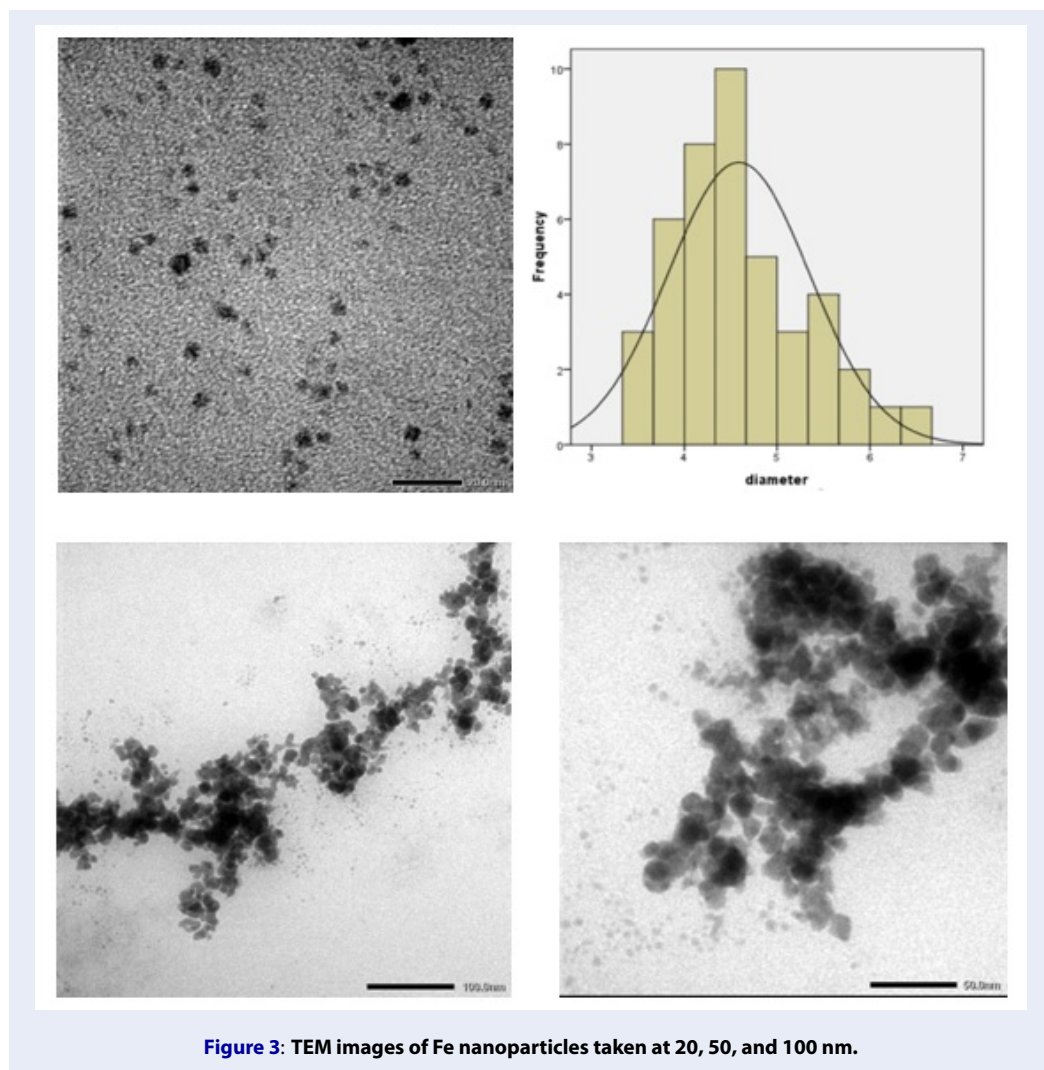
The authors declare that there are no conflicts of interest regarding the publication of this paper.

## AUTHOR'S CONTRIBUTION

Co Thanh Thien has conceived of the present idea, carried out and written the manuscript. Le Dinh Khoi, Le Van De and Doan Thi Nhu Thuy carried out the experiments and analyzed all the samples.

## ACKNOWLEDGMENT

This research is funded by Vietnam National University Ho Chi Minh City (VNU-HCM) under grant number C2019-18-13.



## REFERENCES

- Romero NA, Nicewicz DA. Organic Photoredox Catalysis. *Chem Rev.* 2016;116(17):10075–10166. PMID: 27285582. Available from: <https://doi.org/10.1021/acs.chemrev.6b00057>.
- Hiên TT, Anh LH, Thiện PH, Thành ND. Preparation of activated carbons from coffee husks by hydrothermal carbonization method and application in Methylene Blue dye removal. *Vietnam J Catal Adsorpt.* 2019;8(4):1–9. Available from: <http://chemeng.hust.edu.vn/jca/images/Paper/4-2019/4-2019-p001-009.pdf>.
- Kuan CC, Chang SY, Schroeder SLM. Fenton-like oxidation of 4-chlorophenol: Homogeneous or heterogeneous. *Ind Eng Chem Res.* 2015;54(33):8122–8129. Available from: <https://doi.org/10.1021/acs.iecr.5b02378>.
- Hoan NTV, Minh NN, Nhi TTK, Van Thang N, Tuan VA, Nguyen VT, et al. TiO<sub>2</sub>/Diazonium/graphene oxide composites: Synthesis and visible-light-driven photocatalytic degradation of methylene blue. *J Nanomater.* 2020;2020:1–15. Available from: <https://doi.org/10.1155/2020/4350125>.
- Quan GC, Le TK. Preparation of magnetic photo-Fenton catalysts based on CuFe<sub>2</sub>O<sub>4</sub> by the starch-assisted sol-gel method. *Sci. Technol Dev J - Nat Sci.* 2017;5:102–109. Available from: <https://doi.org/10.32508/stdjns.v1i15.541>.
- Linh HN, Ho HTN. Bio-Electro-Fenton: a novel method for treating leachate in Da Phuoc Landfill, Vietnam. *Sci Technol Dev J.* 2020;23(1):461–469. Available from: <https://doi.org/10.32508/stdj.v23i1.1736>.
- Saufi H, El Alouani M, Alehyen S, El Achouri M, Aride J, Taibi M. Photocatalytic Degradation of Methylene Blue from Aqueous Medium onto Perlite-Based Geopolymer. *Int J Chem Eng.* 2020;2020:1–7. Available from: <https://doi.org/10.1155/2020/9498349>.
- Phan CN, Phan TTN, Pham TH. Heterogeneous Fenton-like LFO catalyst for the degradation of organic pollutant in wastewater. *Vietnam J Catal Adsorpt.* 2019;8(4):110–115. Available from: <http://chemeng.hust.edu.vn/jca/images/Paper/4-2019/4-2019-p110-115.pdf>.
- Ayodele OB, Lim JK, Hameed BH. Pillared montmorillonite supported ferric oxalate as heterogeneous photo-Fenton catalyst for degradation of amoxicillin. *Appl Catal A Gen.* 2012;413(414). Available from: <https://doi.org/10.1016/j.apcata.2011.11.023>.
- Li H, Zhang H, Long J, Zhang P, Chen Y. Combined Fenton process and sulfide precipitation for removal of heavy metals from industrial wastewater: Bench and pilot scale studies focusing on in-depth thallium removal. *Front Environ Sci Eng.* 2019;13(4):1–12. Available from: <https://doi.org/10.1007/s11783-019-1130-7>.

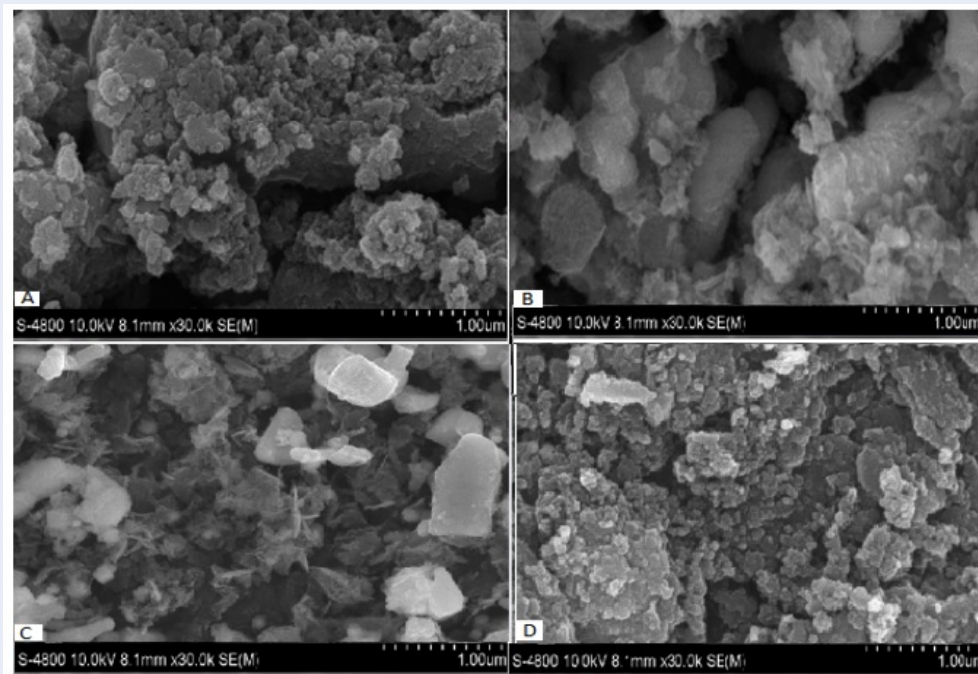


Figure 4: SEM images of: A) Fe-Al<sub>2</sub>O<sub>3</sub>, B) Fe-C, C) Fe-ZnO, and D) Fe-Bent. The images were taken at 1.0 μm.

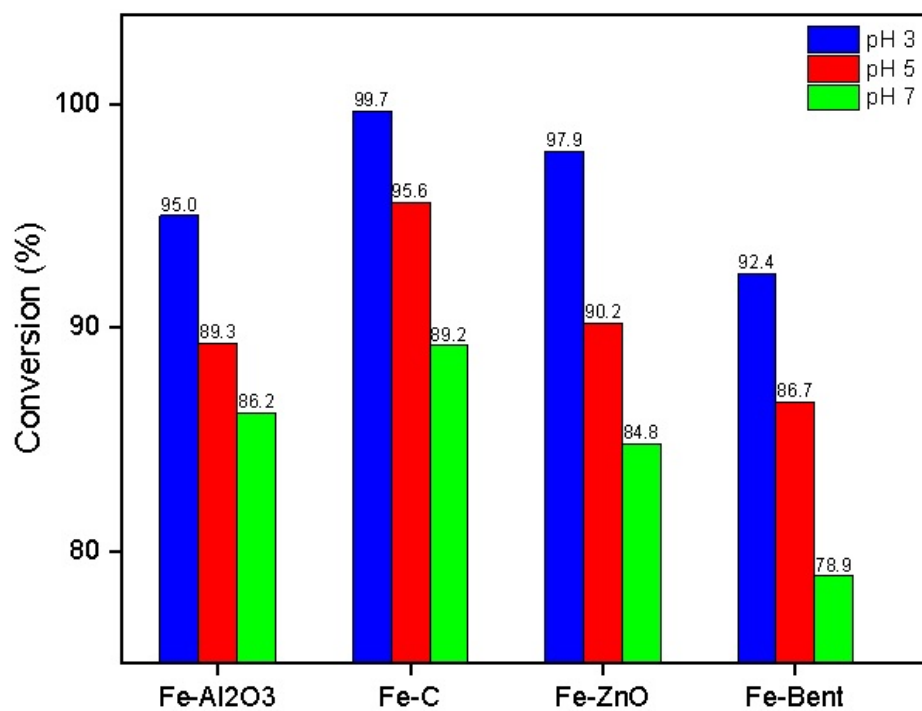


Figure 5: Catalytic activities of Fe-X over MB conversion. Reaction condition: 5 mol% of catalyst at pH 3, pH 5, and pH 7; [MB] = 40 mg/L; reaction time was 60 min.

11. Fu N, Ren XC, Wan JX. Preparation of ag-coated SiO<sub>2</sub>@TiO<sub>2</sub> core-shell nanocomposites and their photocatalytic applications towards phenol and methylene blue degradation. *J Nanomater.* 2019;2019:1–8. Available from: <https://doi.org/10.1155/2019/8175803>.
12. Rodríguez A, Ovejero G, Sotelo JL, Mestanza M, García J. Heterogeneous fenton catalyst supports screening for mono azo dye degradation in contaminated wastewaters. *Ind Eng Chem Res.* 2010;49(2):498–505. Available from: <https://doi.org/10.1021/ie901212m>.
13. Song P, Liu L, Wang AJ, Zhang X, Zhou SY, Feng JJ. One-pot synthesis of platinum-palladium-cobalt alloyed nanoflowers with enhanced electrocatalytic activity for ethylene glycol oxidation. *Electrochim Acta.* 2015;164:323–329. Available from: <https://doi.org/10.1016/j.electacta.2015.02.229>.
14. Mathiyarasu J, Phani KLN. Carbon-Supported Palladium-Cobalt-Noble Metal (Au, Ag, Pt) Nanocatalysts as Methanol Tolerant Oxygen-Reduction Cathode Materials in DMFCs. *J Electrochem Soc.* 2007;154(11):1100–1105. Available from: <https://doi.org/10.1149/1.2772417>.
15. Kim P, Joo JB, Kim W, Kim J, Song IK, Yi J. NaBH<sub>4</sub>-assisted ethylene glycol reduction for preparation of carbon-supported Pt catalyst for methanol electro-oxidation. *J Power Sources.* 2006;160(2):987–990. Available from: <https://doi.org/10.1016/j.jpowsour.2006.02.050>.
16. Chen H, Luo H, Lan Y, Dong T, Hu B, Wang Y. Removal of tetracycline from aqueous solutions using polyvinylpyrrolidone (PVP-K30) modified nanoscale zero valent iron. *J Hazard Mater.* 2011;192(1):44–53. Available from: <https://doi.org/10.1016/j.jhazmat.2011.04.089>.
17. Domenzain-Gonzalez J, Castro-Arellano JJ, Galicia-Luna LA, Lartundo-Rojas L. Photo-Fenton Degradation of RB5 Dye in Aqueous Solution Using Fe Supported on Mexican Natural Zeolite. *Int J Photoenergy.* 2019;2019:1–15. Available from: <https://doi.org/10.1155/2019/4981631>.